ROYAL SOCIETY OF CHEMISTRY

PAPER

Check for updates

Performance enhancement of a ZnMgO film UV photodetector by HF solution treatment†

Xing Chen, (ID) Kewei Liu,* Xiao Wang, Binghui Li, Zhenzhong Zhang, Xiuhua Xie and Dezhen Shen*

Oxygen adsorption and desorption processes can strongly slow down the response speed of ZnO-based ultraviolet photodetectors. Surface passivation of ZnO-based films is a common method to increase the response speed, but the effect of the traditional passivation technology is usually not very obvious, and often accompanies a decrease in responsivity. Herein we propose a new method to overcome this problem: treating ZnMgO UV photodetectors with HF solution. Interestingly, after treatment with HF solution, the 90−10% decay time of the device is decreased by more than one order of magnitude (from 4.6 ms to 0.34 ms), which can be attributed to the enhancement of the oxygen adsorption speed on the surface of ZnMgO due to the F-modified surface. Moreover, the dark current is decreased from 0.7 pA to 0.4 pA at a bias of 10 V and the responsivity is increased from 145 A W^{-1} to 326 A W^{-1}. Thus, chemical treatment with HF solution should be a useful and effective method for improving the performance of ZnMgO UV photodetectors.

Introduction

Ultraviolet (UV) photodetectors have wide applications in environmental monitoring, flame and radiation detection, astronomical studies, and optical communications.[1–6] In recent years, UV detectors based on wide bandgap semiconductors (such as diamond,[7–9] SiC,[10–12] GaN[13–15] and ZnO[16–18]) have received more and more attention due to their intrinsic visible or solar blindness, high radiation hardness, no need for any filters or refrigeration, and so on. Among the wide-bandgap semiconductors, ZnO has many unique properties such as a relatively lower defect density, a higher saturated carrier drift rate, low cost, and a wide band-gap tuning range by alloying ZnO with MgO (3.37 eV–7.8 eV).[16–20] Therefore, ZnO and its ternary alloy ZnMgO have been regarded as some of the most promising materials for the fabrication of high performance UV photodetectors.

To date, ZnO-based UV photodetectors with different device structures have been reported, such as p–n junction, Schottky junction and metal–semiconductor–metal (MSM) structures.[21–26] According to previous reports, the performance of these devices is significantly dependent on the properties of ZnO-based

semiconductor materials. In particular, ZnO shows a strong adsorption/desorption behavior of oxygen on the surface, which could increase the responsivity and decrease the dark current of the ZnO-based UV photodetectors.[21,22] However, these adsorption/desorption processes of oxygen on the surface of ZnO always lead to a long rise/decay time of bare ZnO UV photodetectors, which hinders their practical applications.[22] In order to overcome this drawback, several methods have been developed to passivate the surface states on ZnO which could be responsible for the adsorption of oxygen,[27–33] such as surface modification by nanomaterials,[28,29] surface treatment of SiO_2,[30] surface modification by organic materials,[31,33] and surface treatment of H_2O_2.[32] Although the response speed of ZnO-based UV photodetectors could be more or less improved by using the above-mentioned methods, it was often accompanied by a decrease in the photocurrent and an increase in the dark current.[30,32,34] The key reason for this phenomenon is that the previous surface treatment methods just reduce the surface states density and thus decrease the amount of absorbed oxygen. Therefore, it is still a big challenge to develop an effective surface treatment method to improve the response speed, increase the responsivity and decrease the dark current simultaneously.[22,23]

We note that treatment with HF solution can modify the surface properties of oxide semiconductors, which could enhance their ability for oxygen adsorption and desorption.[35,36] In other words, the surface modification of oxide materials by HF solution treatment could not only reduce the surface state density, but could also increase the speed of oxygen adsorption and desorption. It is thus expected that the response speed of

State Key Laboratory of Luminescence and Applications, Changchun Institute of Optics, Fine Mechanics and Physics, Chinese Academy of Sciences, 3888 Dongnanhu Road, Changchun 130033, P. R. China. E-mail: liukw@ciomp.ac.cn, shendz@ciomp.ac.cn

ZnO-based photodetectors can be improved by HF solution treatment without any degradation of the responsivity and the dark current. Additionally, a large amount of F on the surface of ZnO may be beneficial for improving the responsivity and reducing the dark current of the devices. In this paper, ZnMgO film UV photodetectors treated with HF solution have been demonstrated on c-Al$_2$O$_3$ substrates by plasma-assisted molecular beam epitaxy (P-MBE). After the HF solution treatment, the 90–10% decay time of the ZnMgO photodetectors was decreased by more than one order of magnitude (from 4.6 ms to 0.34 ms). Moreover, the responsivity was increased from 145 A W^{-1} to 326 A W^{-1}, and the dark current was decreased from 0.7 pA to 0.4 pA at a bias of 10 V. The mechanism of the property change has been discussed. Our findings indicated that this simple HF solution treatment method can be used to improve the performance (response speed, responsivity, and dark current) of ZnO-based UV photodetectors.

Experimental

Synthesis and characterization of ZnMgO films

ZnMgO films were fabricated on c-Al$_2$O$_3$ substrates by a P-MBE system, and 6N-purity zinc and 5N-purity magnesium held in thermal Knudsen cells and 5N-purity O$_2$ activated in a radio frequency plasma source were selected as precursors. Prior to growth, the substrates were treated with N$_2$ at 950 °C for 60 min to remove possible absorbed contaminants. During growth, the chamber pressure was maintained at 10^{-3} Pa and the substrate temperature was kept at 450 °C. The radio frequency power was fixed at 300 W with an O$_2$ flow rate of 1.1 sccm. The samples were characterized by using scanning electron microscopy (SEM) (HITACHI S-4800), energy dispersive X-ray spectrometry (EDS) (GENESIS 2000 XMS60S), X-ray diffraction (XRD) using Cu Kα radiation (λ = 0.154 nm) with an area detector and UV-Vis transmission spectrometry (Shimadzu UV-3101PC). X-ray photoelectron spectra (XPS) were recorded using an ESCALAB Mk II (Vacuum Generators) spectrometer and Al Kα X-rays (240 W). The binding energies were calibrated against the C 1s signal (284.6 eV) of adventitious carbon. Photoluminescence (PL) measurements were carried out using a JY-630 micro-Raman spectrometer employing the 325 nm line of a He–Cd laser as the excitation source.

Fabrication and characterization of the photodetectors

The schematic illustration of the fabrication of the device is shown in Fig. 1. After the epitaxy of the ZnMgO films on the c-sapphire, Au interdigital electrodes (20 nm thick) were prepared on all films through photolithography and a wet etching procedure to form MSM photodetectors. After that, the photodetectors were immersed in HF solution for 0.5 second at room temperature. The current–voltage (I–V) properties were measured by using a semiconductor device analyzer (Agilent B1500A). A 200 W UV enhanced Xe lamp with a monochromator was used to investigate the spectral response properties of the photodetectors. The transient response spectra of the photodetectors were recorded by using an oscilloscope (Tektronix DPO 5104 digital oscilloscope) and a Nd:YAG laser (266 nm).

Results and discussion

The ZnMgO films before and after HF solution treatment (HF: [H$^+$] = 17 mmol L^{-1}) were characterized by SEM, XRD and UV-Vis transmission spectra. For convenience, the ZnMgO treated with HF solution with a concentration of 17 mmol L^{-1} is referred to as ZnMgO–F17. Fig. 2(a) and (b) show the typical top-view SEM images of ZnMgO and ZnMgO–F17 films. Almost no change in the surface morphology of ZnMgO films can be found after the solution treatment. In addition, the cross-sectional SEM images [see the insets of Fig. 2(a) and (b)] indicate that the thickness of both ZnMgO and ZnMgO–F17 films is around 380 nm. The XRD pattern of the samples is shown in Fig. 2(c). Besides the diffraction peak of the c-sapphire substrate, only one diffraction peak located at 2θ = 34.7° can be observed for both the samples, which corresponds to the (0002) orientation of wurtzite ZnMgO. Fig. 2(d) shows the UV-Vis transmission spectra of the films. It is clear that both the films have more than 90% average transmission in the visible region and have a very abrupt absorption edge at around 325 nm. Obviously, the HF solution treatment could not change the surface morphology, thickness, crystal structure, and light transmission of ZnMgO films. Moreover, the EDS result (see Fig. S1, ESI†) indicates that the composition of the films is Zn$_{0.81}$Mg$_{0.19}$O. Within the limits of experimental error, there is no difference between the films before and after HF modification.

In order to confirm the existence of F on the surface of ZnMgO–F17 films, the XPS spectra were measured and the binding energies were calibrated using the C 1s peak (284.6 eV) as the reference from the surface adventitious carbon. Fig. 3(a) shows the XPS survey spectrum of the ZnMgO–F17 film and all the peaks can be ascribed to Zn, O, Mg, F and C. The high-resolution F 1s spectrum has been acquired and it is shown in Fig. 3(b). The two peaks located at 689.0 eV and 684.8 eV can be attributed to the fluoride ions both in the ZnMgO lattice and on the surface of the oxide film.[37,38] In order to further confirm the
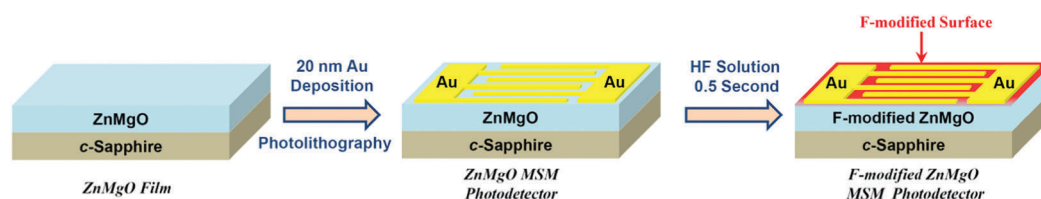

Fig. 1 Schematic illustration of the fabrication of F-modified ZnMgO MSM photodetectors.
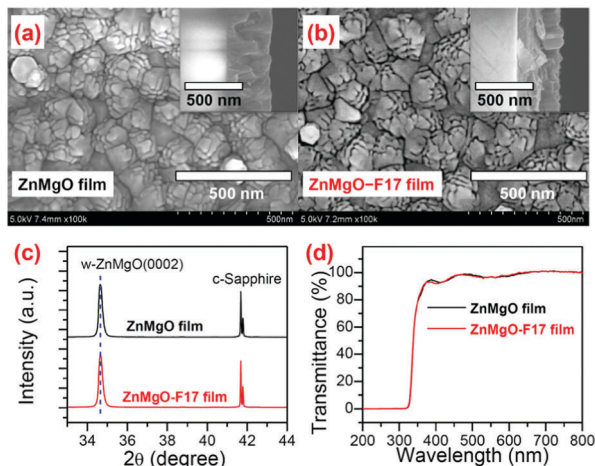
Fig. 2 (a and b) SEM images of ZnMgO films. The insets are the cross sectional SEM images of ZnMgO films. (c) XRD patterns of ZnMgO films. (d) UV-Vis transmission spectra of ZnMgO films.

presence of Zn–F and Mg–F bonds, high resolution Zn 2p$_{3/2}$ and Mg 2p XPS spectra of ZnMgO films treated with a series of HF solutions with different concentrations were recorded as shown in Fig. 3(c) and (d). A positive shift of both Zn 2p$_{2/3}$ and Mg 2p

binding energies can be clearly observed by increasing the F concentration. The XPS results suggest that F atoms should substitute O atoms and form Zn–F and Mg–F bonds.[39,40]

In order to further investigate the effect of HF solution treatment on the photoresponse properties of ZnMgO films, the performance of the ZnMgO MSM photodetectors has been measured. The I–V characteristics in the dark are shown in Fig. 4(a). After treatment with HF, the dark current decreases from 0.7 pA to 0.4 pA at a bias of 10 V. Fig. 4(b) shows the spectral responses of the devices before and after HF solution treatment under a bias of 10 V. Obviously, the devices display a visible–blind photoresponse with a cutoff wavelength of ∼345 nm. The response peak with a responsivity of 145 A W^{-1} is located at ∼325 nm, which is in good agreement with the UV-Vis transmission spectra of the ZnMgO films. After treatment with HF, the peak responsivity of the device increases from 145 A W^{-1} to 326 A W^{-1}.

The transient response (I–t curves) to 266 nm laser of the devices is shown in Fig. 5. The 90–10% decay time (t-decay: defined as the time for the current dropping from 90% to 10% of the peak value) of the ZnMgO film UV photodetector is around 4.6 ms, and the HF solution treatment could lead to a large decrease in response time by more than one order of magnitude (from 4.6 ms to 0.34 ms).
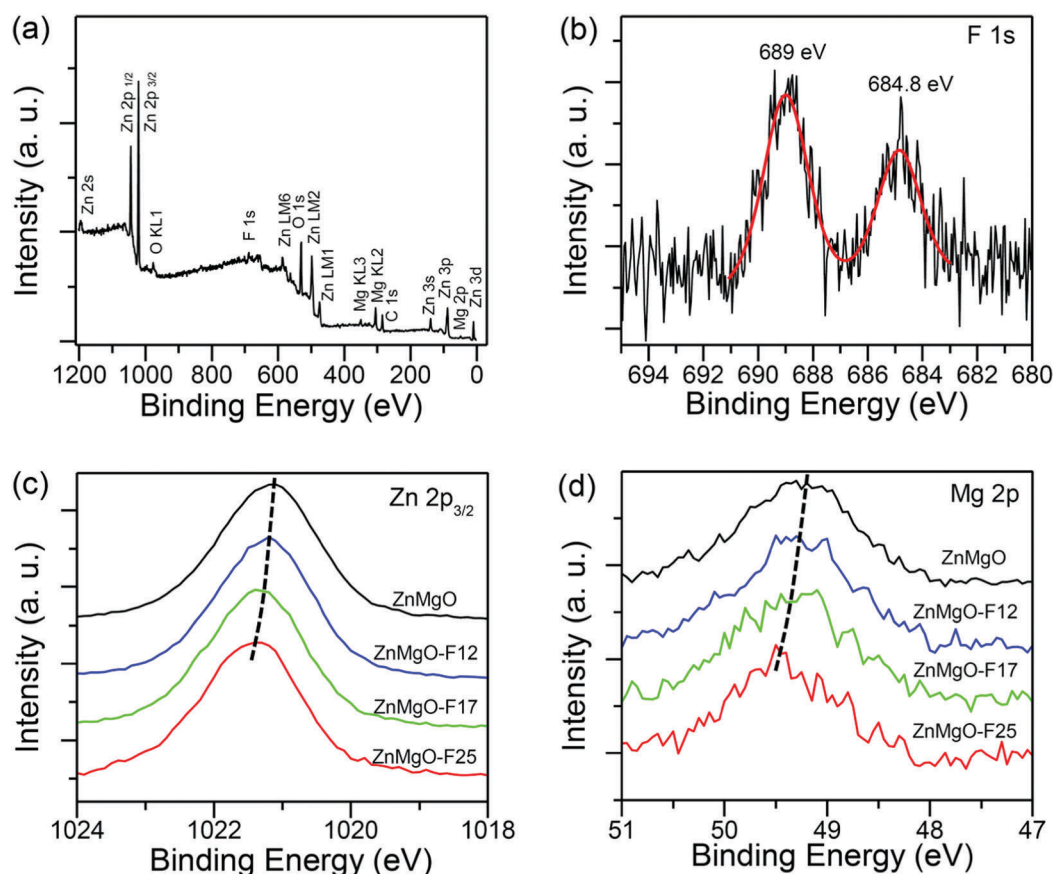

Fig. 3 (a) XPS survey spectrum and (b) high-resolution F 1s spectrum of the ZnMgO–F17 film. (c) High-resolution Zn 2p$_{3/2}$ spectra of films. (d) High-resolution Mg 2p spectra of films. The films were modified by immergence in a series of HF solutions for 0.5 second. The unmodified film was defined as ZnMgO, and the modified films were defined as ZnMgO–F12 (HF: [H$^+$] = 12 mmol L^{-1}), ZnMgO–F17 (HF: [H$^+$] = 17 mmol L^{-1}) and ZnMgO–F25 (HF: [H$^+$] = 25 mmol L^{-1}), respectively.
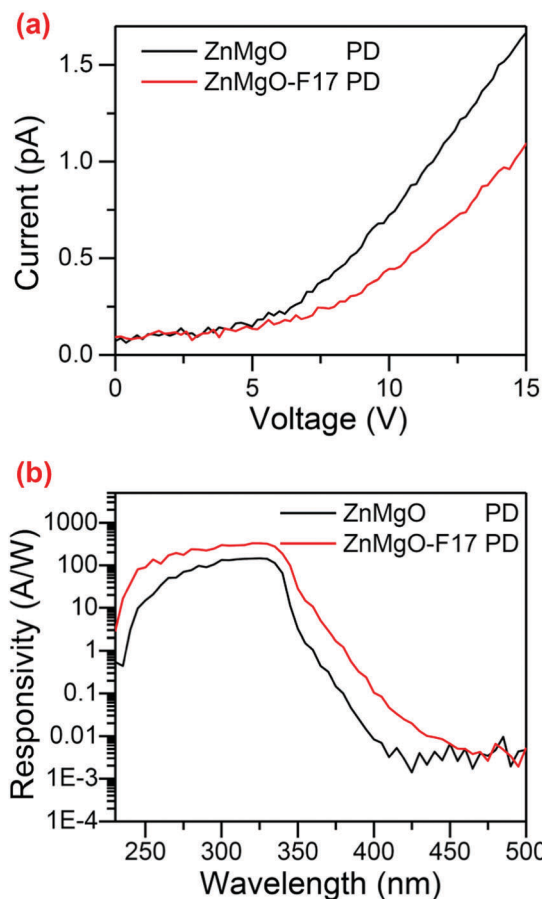
Fig. 4 (a) $I-V$ characteristics of devices in the dark. (b) Spectral responses of the devices under a bias of 10 V. The devices were modified by immergence in HF solutions for 0.5 second. The unmodified device was defined as ZnMgO PD, and the modified device was defined as ZnMgO–F17 PD (HF: $[H^+]$ = 17 mmol L^{-1}).

Fig. 5 Decay edge of the current response at a bias of 10 V.
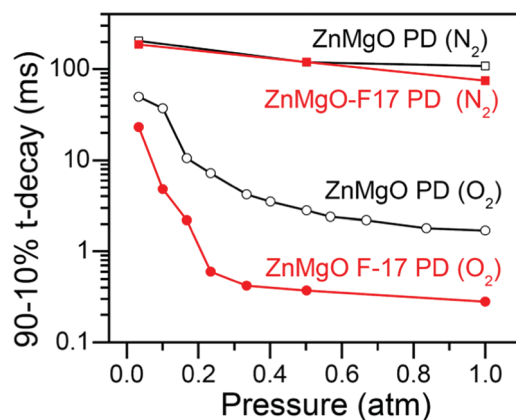
Fig. 6 90–10% decay time of the devices as a function of atmosphere and pressure.

In order to investigate the effect of surface treatment on the O_2 adsorption/desorption processes, the 90–10% decay times of the devices as a function of atmosphere and pressure were measured as shown in Fig. 6. In a N_2 atmosphere, the devices with and without HF solution treatment have the similar decay time, which decreases slightly by increasing the pressure from 0.05 to 1 atm. In contrast, the decay time of the devices in an O_2 atmosphere decreases sharply with the increase of O_2 pressure from 0.05 to 0.3 atm. As the pressure is increased further, the decay time decreases slightly. Obviously, the response speed of the devices in an O_2 atmosphere is much quicker than that in a N_2 atmosphere. More interestingly, HF solution treatment could remarkably increase the response speed of ZnMgO UV photodetectors in an O_2 atmosphere.

Table 1 shows the comparison of the photoresponse parameters between the ZnO (ZnMgO) based photodetectors which were treated using various methods. It can be seen that several methods could reduce the decay time for about one order of magnitude, however the decay time is still not low enough.[22,28,29] ZnMgO films treated with oxygen plasma could gain a very fast response speed, but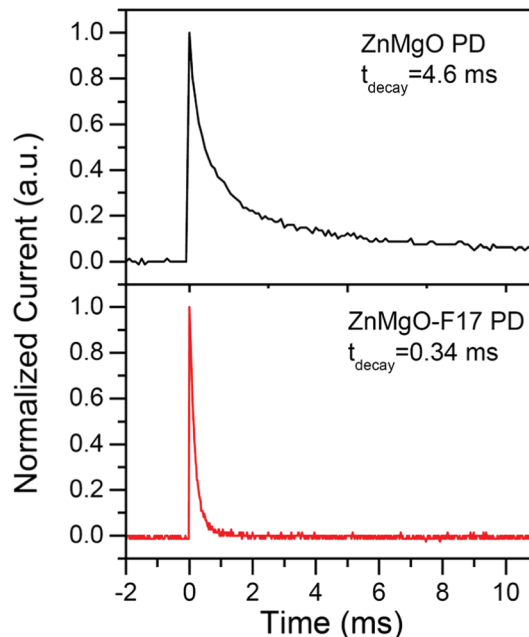 the responsivity of the device is obviously lower than other devices.[42] Moreover, the device has a relatively high dark current. The response speed of ZnO-based UV photodetectors could be more or less improved by treatment with SiO_2 or H_2O_2, but it was accompanied by a decrease in the photocurrent.[30,32] As compared to previous reports, our F-modified ZnMgO photodetector has a relatively quicker response speed, higher responsivity and a lower dark current. To explain these high comprehensive performances of F-modified devices, a model taking into account surface adsorption and desorption together with electron–hole activities inside ZnMgO is proposed. Fig. 7 shows the schematic views of the UV photoresponse process of ZnMgO and ZnMgO–F17 PDs. ZnO and ZnMgO are intrinsic n-type semiconductor materials and the electrons play a main role in making the contribution to conductivity. In the dark environment, oxygen molecules are adsorbed on the surface of the ZnMgO film and capture the free electrons. As a result,

Table 1 Performance comparison of the ZnO-based photodetectors treated using different methods

Structure	Surface treatment		Decay time (s)	Responsivity (A W^{-1})	I-dark (nA)	Bias (V)	Ref.
ZnO 1-D	CuPc[a]	Before	398[d]	$\sim 1.5 \times 10^6$	~ 80	1	22
		After	3[d]	2.9×10^6	~ 0.1		
ZnO 1-D	ZnO QDs[b]	Before	4.66[d]	~ 0.9	~ 3	5	28
		After	0.44[d]	~ 10	~ 5		
ZnO 1-D arrays	Al nanoparticles	Before	0.85[d]	0.12	50	5	29
		After	0.035[d]	1.59	200		
ZnO 1-D arrays	SiO$_2$	Before	33.1[d]	0.1	~ 500	5	30
		After	13.9[d]	0.03	—		
ZnO 1-D arrays	C$_6$H$_{12}$N$_4$[c]	Before	0.59[e]	0.05	~ 5.3	20	31
		After	0.13[e]	33.33	~ 7.1		
ZnO film	HCl	Before	—	0.05	3.83×10^4	10	41
		After	—	0.14	8.46×10^4		
ZnMgO film	Oxygen plasma	Before	—	0.56	8×10^5	-4	42
		After	$4.78 \times 10^{-7\,e}$	4.21	1.1×10^4		
ZnMgO film	H$_2$O$_2$	Before	~ 4[e]	14	9×10^{-3}	1	32
		After	~ 1[e]	4	6×10^{-4}		
ZnMgO film	HF	Before	$4.6 \times 10^{-3\,e}$	145	7.2×10^{-4}	10	This work
		After	$3.4 \times 10^{-4\,e}$	326	4.4×10^{-4}		

[a] Copper phthalocyanine. [b] ZnO quantum dots. [c] Hexamethylenetetramine. [d] These data are decay time constants (τ) which are defined as the time to recover $1/e$ of the maximum photocurrent. [e] These data are 90–10% decay time.
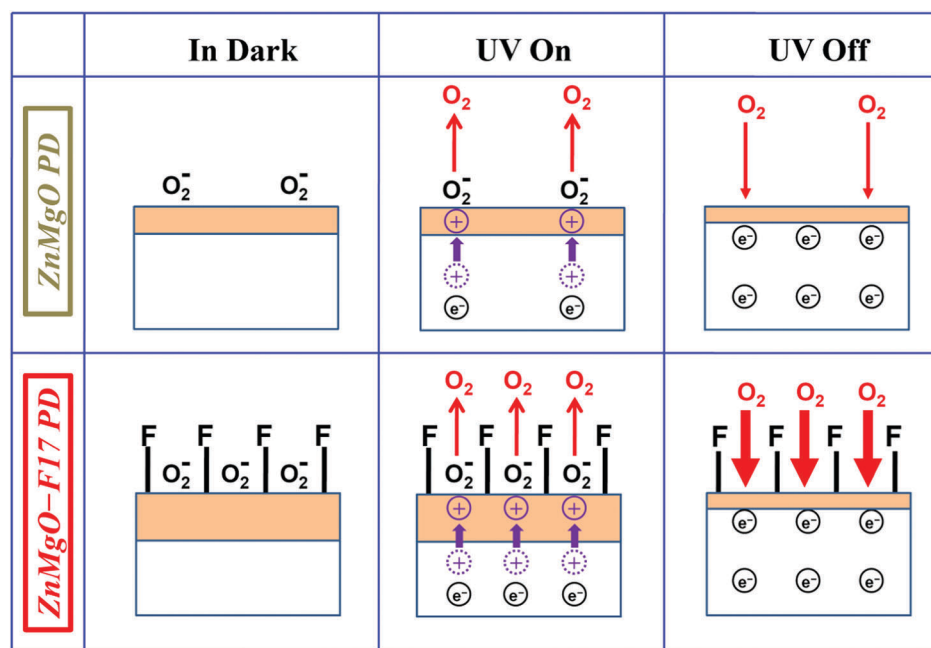

Fig. 7 Schematic views of the UV photoresponse process of ZnMgO and ZnMgO–F17 PDs.

a depletion layer with low conductivity is created near the surface of the film. After HF solution treatment, large amounts Zn–F or Mg–F can be formed on the ZnMgO surface, and the O$_2$ adsorption heat of (Zn, Mg)–F is much larger than that of (Zn, Mg)–O due to the higher electronegativity of F.[35] Therefore, the F-modified surface could adsorb more O$_2$ molecules, and the thickness of the depletion layer is thus increased, resulting in a decrease in dark current.

When the devices are illuminated with UV light, the electrons and holes are generated in the ZnMgO film. Then, the photogenerated electrons and holes are separated and drift to electrodes. Meanwhile, some of these photogenerated holes can migrate to oxygen related hole-trap states on the film surface due to the build-in electric field in the depletion region, discharging the chemisorbed oxygen ions and then desorbing them. According to the previous reports, these oxygen related hole-trap states can lead to a photoconductive gain. The F-modified surface could induce more oxygen related hole-trap states due to the strong O$_2$ adsorption ability, which thus can be responsible for the larger responsivity. After turning off the UV light, the oxygen molecules are reabsorbed on the surface of ZnMgO and capture the free electrons more quickly, presumably due to decreased activation energy of oxygen adsorption for oxygen adsorption on the surface.[43] Thus the smaller t-decay is achieved for the ZnMgO–F17 PD.

The photoresponse parameters between the devices which were treated with different $H^+ \bullet (HF)$ concentrations and treatment times are shown in Table S1 and Fig. S2 (ESI†). With the increase of the concentration of $H^+ \bullet (HF)$ or treatment time, the t-decay decreases, the photoresponse increases, and the dark current decreases. The photoresponse parameters between the new devices and the devices which were stored in an electronic humidity control box for 4 months are shown in Fig. S3 (ESI†). It can be seen that the stability of our devices (the unmodified device and the F-modified device) is relatively good.

In addition, the effect of HF treatment on the photoluminescence (PL) properties of ZnMgO films was investigated as shown in Fig. S4 in the ESI.† According to the previous work,[44] the visible emission of PL can be attributed to the oxygen vacancies. In our work, the visible emission has no significant change when the films are treated with HF. This suggests that the oxygen vacancies of the ZnMgO films are not significantly changed.

It must be mentioned here that H^+ on the surface of ZnMgO may be another reason for the enhancement of performance. In order to clarify this problem, we have treated the devices with different acid solutions. It can be found that the performance of ZnMgO photodetectors treated with other solutions did not show any obvious change. Therefore, the effect of H^+ on the performance improvement can be ignored in this work (see the ESI,† Table S1).

Conclusions

In summary, we demonstrated a performance enhancement of ZnMgO photodetectors through HF solution treatment. By immersing ZnMgO photodetectors in HF solution, the surface of the films was modified by the F element. As a result, the 90–10% decay time of the F-modified ZnMgO photodetector is decreased by more than one order of magnitude (from 4.6 ms to 0.34 ms). The decrease in the decay time is associated with the enhancement of the oxygen adsorption speed on the surface of ZnMgO due to the F-modified surface. Moreover, the responsivity was increased from 145 A W^{-1} to 326 A W^{-1}, and the dark current was decreased from 0.7 pA to 0.4 pA at a bias of 10 V. Large amounts of Zn–F or Mg–F on the ZnMgO surface should be responsible for the performance enhancement after HF treatment. Our findings suggest that chemical treatment with HF should be an effective method for improving the performance of the ZnMgO UV photodetector, which paves a new way for the fabrication of oxide photodetectors with high comprehensive performance.

Conflicts of interest

There are no conflicts to declare.

Acknowledgements

Notes and references

1 C. Soci, A. Zhang, B. Xiang, S. A. Dayeh, D. P. R. Aplin, J. Park, X. Y. Bao, Y. H. Lo and D. Wang, *Nano Lett.*, 2007, **7**, 1003–1009.

2 K. W. Liu, M. Sakurai and M. Aono, *Sensors*, 2010, **10**, 8604–8634.

3 X. Liu, L. L. Gu, Q. P. Zhang, J. Y. Wu, Y. Z. Long and Z. Y. Fan, *Nat. Commun.*, 2014, **5**, 4007.

4 M. M. Fan, K. W. Liu, X. Chen, X. Wang, Z. Z. Zhang, B. H. Li and D. Z. Shen, *ACS Appl. Mater. Interfaces*, 2015, **7**, 20600–20606.

5 X. Chen, K. W. Liu, Z. Z. Zhang, C. R. Wang, B. H. Li, H. F. Zhao, D. X. Zhao and D. Z. Shen, *ACS Appl. Mater. Interfaces*, 2016, **8**, 4185–4191.

6 P. N. Ni, C. X. Shan, S. P. Wang, X. Y. Liu and D. Z. Shen, *J. Mater. Chem. C*, 2013, **1**, 4445–4449.

7 M. Y. Liao, Y. Koide and J. Alvarez, *Appl. Phys. Lett.*, 2005, **87**, 022105.

8 M. Y. Liao and Y. Koide, *Appl. Phys. Lett.*, 2006, **89**, 113509.

9 J. Chen, S. Lourette, K. Rezai, T. Hoelzer, M. Lake, M. Nesladek, L. S. Bouchard, P. Hemmer and D. Budker, *Appl. Phys. Lett.*, 2017, **110**, 011108.

10 X. P. Chen, H. L. Zhu, J. F. Cai and Z. Y. Wua, *J. Appl. Phys.*, 2007, **102**, 024505.

11 A. Sciuto, F. Roccaforte, S. Di Franco, V. Raineri and G. Bonanno, *Appl. Phys. Lett.*, 2006, **89**, 081111.

12 S. Yang, D. Zhou, H. Lu, D. J. Chen, F. F. Ren, R. Zhang and Y. D. Zheng, *IEEE Photonics Technol. Lett.*, 2016, **28**, 1185–1188.

13 R. Calarco, M. Marso, T. Richter, A. I. Aykanat, R. Meijers, A. V. Hart, T. Stoica and H. Luth, *Nano Lett.*, 2005, **5**, 981–984.

14 X. L. Zhang, B. D. Liu, Q. Y. Liu, W. J. Yang, C. M. Xiong, J. Li and X. Jiang, *ACS Appl. Mater. Interfaces*, 2017, **9**, 2669–2677.

15 J. Lahnemann, M. Den Hertog, P. Hille, M. de la Mata, T. Fournier, J. Schormann, J. Arbiol, M. Eickhoff and E. Monroy, *Nano Lett.*, 2016, **16**, 3260–3267.

16 Y. N. Hou, Z. X. Mei and X. L. Du, *J. Phys. D: Appl. Phys.*, 2014, **47**, 283001.

17 M. M. Fan, K. W. Liu, X. Chen, Z. Z. Zhang, B. H. Li, H. F. Zhao and D. Z. Shen, *J. Mater. Chem. C*, 2015, **3**, 313–317.

18 M. M. Fan, K. W. Liu, Z. Z. Zhang, B. H. Li, X. Chen, D. X. Zhao, C. X. Shan and D. Z. Shen, *Appl. Phys. Lett.*, 2014, **105**, 011117.

19 P. K. Shrestha, Y. T. Chun and D. P. Chu, *Light: Sci. Appl.*, 2015, **4**, e259.

20 Z. G. Ju, C. X. Shan, D. Y. Jiang, J. Y. Zhang, B. Yao, D. X. Zhao, D. Z. Shen and X. W. Fan, *Appl. Phys. Lett.*, 2008, **93**, 173505.

21 H. Kind, H. Q. Yan, B. Messer, M. Law and P. D. Yang, *Adv. Mater.*, 2002, **14**, 158–160.

10650 | *J. Mater. Chem. C*, 2017, **5**, 10645–10651

This journal is © The Royal Society of Chemistry 2017

22 Q. Chen, H. Y. Ding, Y. K. Wu, M. Q. Sui, W. Lu, B. Wang, W. M. Su, Z. Cui and L. W. Chen, *Nanoscale*, 2013, **5**, 4162–4165.

23 Z. Alaie, S. M. Nejad and M. H. Yousefi, *Mater. Sci. Semicond. Process.*, 2015, **29**, 16–55.

24 L. Q. Qin, C. Shing, S. Sawyer and P. S. Dutta, *Opt. Mater.*, 2011, **33**, 359–362.

25 N. Kouklin, *Adv. Mater.*, 2008, **20**, 2190–2194.

26 H. Y. Chen, K. W. Liu, X. Chen, Z. Z. Zhang, M. M. Fan, M. M. Jiang, X. H. Xie, H. F. Zhao and D. Z. Shen, *J. Mater. Chem. C*, 2014, **2**, 9689–9694.

27 G. Cheng, X. H. Wu, B. Liu, B. Li, X. T. Zhang and Z. L. Du, *Appl. Phys. Lett.*, 2011, **99**, 203105.

28 C. X. Wu, Z. J. He, J. F. Lu, J. Dai and C. X. Xu, *RSC Adv.*, 2016, **6**, 687–691.

29 J. F. Lu, C. X. Xu, J. Dai, J. T. Li, Y. Y. Wang, Y. Lin and P. L. Li, *Nanoscale*, 2015, **7**, 3396–3403.

30 S. H. Lee, S. H. Kim and J. S. Yu, *Nanoscale Res. Lett.*, 2016, **11**, 333.

31 A. Rostami, M. Dolatyari, E. Amini, H. Rasooli, H. Baghban and S. Miri, *ChemPhysChem*, 2013, **14**, 554–559.

32 Y. X. Zhu, K. W. Liu, X. Wang, J. L. Yang, X. Chen, X. H. Xie, B. H. Li and D. Z. Shen, *J. Mater. Chem. C*, 2017, **5**, 7598–7602.

33 Z. W. Jin and J. Z. Wang, *J. Mater. Chem. C*, 2014, **2**, 1966–1970.

34 S. K. Tzeng, M. H. Hon and I. C. Leu, *Mater. Chem. Phys.*, 2013, **139**, 963–967.

35 Y. B. Luan, L. Q. Jing, Y. Xie, X. J. Sun, Y. J. Feng and H. G. Fu, *ACS Catal.*, 2013, **3**, 1378–1385.

36 J. S. Park and W. Choi, *Langmuir*, 2004, **20**, 11523–11527.

37 S. Ahmad, M. Kharkwal, Govind and R. Nagarajan, *J. Phys. Chem. C*, 2011, **115**, 10131–10139.

38 J. C. Yu, J. G. Yu, W. K. Ho, Z. T. Jiang and L. Z. Zhang, *Chem. Mater.*, 2002, **14**, 3808–3816.

39 S. Ilican, M. Caglar, S. Aksoy and Y. Caglar, *J. Nanomater.*, 2016, **2016**, 1–9.

40 Y. J. Choi, K. M. Kang and H. H. Park, *Sol. Energy Mater. Sol. Cells*, 2015, **132**, 403–409.

41 S. P. Chang, R. W. Chuang, S. J. Chang, C. Y. Lu, Y. Z. Chiou and S. F. Hsieh, *Thin Solid Films*, 2009, **517**, 5050–5053.

42 J. D. Hwang, S. Y. Wang and S. B. Hwang, *J. Alloys. Compd.*, 2016, **656**, 618–621.

43 J. X. Zhao, C. R. Cabrera, Z. H. Xia and Z. F. Chen, *Carbon*, 2016, **104**, 56–63.

44 E. Polydorou, A. Zeniou, D. Tsikritzis, A. Soultati, I. Sakellis, S. Gardelis, T. A. Papadopoulos, J. Briscoe, L. C. Palilis, S. Kennou, E. Gogolides, P. Argitis, D. Davazogloua and M. Vasilopoulou, *J. Mater. Chem. A*, 2016, **4**, 11844–11858.

This journal is © The Royal Society of Chemistry 2017

J. Mater. Chem. C, 2017, **5**, 10645–10651 | **10651**